ISSN 1392 - 1207. MECHANIKA. 2005. Nr.5(55)

Semi analytical modelling of reinforced concrete members in bending

R. Balevičius
Vilnius Gediminas Technical University, Saulėtekio al. 11, 10223 Vilnius, Lithuania,
E-mail: Robertas.Balevicius@st.vtu.lt

1. Introduction

In recent years, due to rapid development of computer-aided methods, improvement of analytical models and explicit explanation of material properties the reinforced concrete (RC) structures have resulted in longer spans and smaller cross-sections. RC structures are brittle compared to steel structures; consequently, it is very important to describe the behaviour of reinforced concrete under the full range of load conditions and estimate its ultimate strength accurately. In truth, it is difficult in analytical manner to describe effectively the composite behaviour of two completely different materials, concrete and steel, and to consider the time-dependent variation of material properties and effects between both materials. Hence, the analysis of reinforced concrete may be performed choosing between the analytical, code-based methods [1-3] or implementing numerical techniques.

Numerical methods are based on the universal principles enabling us to apply sophisticated mathematical models describing various processes, such as concrete cracking, reinforcement slipping, material nonlinearities, creep, shrinkage, etc. [4-6]. In general case, since a structure is composed of many structural members, and a member is formed by the integration of each section, the nonlinear behaviour of a section causes nonlinear behaviour in the structure. Especially, in the case of beams and columns which are the primary importance members of a frame structure, the problem is non smooth and non convex. In many cases conventional iterative methods of the Newton's type are frequently inefficient when solving a set of nonlinear equations in order to find all possible solutions [5, 7]. Consequently, the main limitation of numerical methods, in great part, are related to computational capabilities due to huge number of unknowns [8], convergence and numerical instability processes, which can have the crucial influence on the obtained results [9]. Hereby, a practical engineer must dispose not only good skill in structural design but the programming-based knowledge is strongly needed in order to perform numerical analysis reliably.

Analytical methods in analysis of RC structures are usually limited by constitutive laws of mathematics, e.g. [10]. Therefore, for developing code methodologies, e.g. [1-3], a large number of empirical expressions and factors that reveal simplification of the actual stress strain state is adopted. These simplifications ensure safe design and allow performing the analysis of RC response directly by formulas without using of programming. The empirical approaches by means of various factors allow to evaluate indirectly different complex effects which are usually not taken into account in numerical analysis and, as a rule, give the possibilities to control correctness of the numerical results.

The extensive analytical and experimental studies of load-deflection responses of RC beams and columns have been reported since the 1960s. In passing, Rozenbliumas [11] proposed the method of complex evaluation of tensile concrete, crack depths and bond-slipping of RC concrete beams. In order to simplify numerical scheme are based the methods in which the analytical moment–curvature relationship is approximately known in advance. This approach has been implemented by Mendis and Darval [12] determining the buckling functions of a column in nonlinear analysis of softening frames. Sheikh [13] has performed an overview of analytical moment-curvature relations for RC columns. Rodriguez-Gutierrez et al. [14] presents the generation biaxial bending moment–axial force–curvature diagrams for reinforced, partially and fully prestressed concrete sections. Hsu [15] proposed some nomenclature of analytical models for linear reinforced members.

Because the structural analysis of RC structures requires great computational effort for iterations and numerical instability due to variation of structural appearance and material properties occur as working stress increases, it is needed to develop the method which allows us to simplify modeling of nonlinear behavior of RC members. Rather than using the layer approach, related to the causes of inaccurate dividing of the cross section into horizontal stripes, the checking of iteration convergence for each and all layers changing of elastic stiffness as well as the searching of the location of neutral axis within the layers, the semi-analytical modeling of RC members in bending is presented in the present research. The proposed technique focuses on the explicit derivation of the internal forces and moments for concrete in tension and compression without the need of the numerical integration. The application of different stress strain relations for compressive concrete and smeared crack approach for tensile concrete is investigated on the basis of the opportunity to find the explicit solution of nonlinear equations. The proposed technique is verified by the comparison of theoretical results with experimental tests data.

2. Stress strain state

2.1. Basic assumptions

In stress strain state formulation, we use the basic assumptions that the plane of cracked sections remains plain, i.e. longitudinal average strain is directly proportional to the distance from neutral axis of zero strain. Perfect bond between reinforcement and concrete in compression is assumed. Tension stiffening effect is simulated relying on smeared crack approach [16].

2.2. Constitutive laws for materials

The stress strain relationships of concrete in uni-

axial compression have been proposed by many researchers. Most of the models, however, are based on test results obtained from their own experiments. Therefore, the results of the models can be subjected to great variation according to test methods and test conditions. The following widely employed stress strain relations of compressive concrete are investigated:

- prEN 1992–1's [1] stress strain curve

$$\sigma_b(\varepsilon_b)=\frac{\dfrac{\varepsilon_b}{\nu_{bR}\varepsilon_{bR}}-\left(\dfrac{\varepsilon_b}{\varepsilon_{bR}}\right)^2}{1+\left(\dfrac{1}{\nu_{bR}}-2\right)\dfrac{\varepsilon_b}{\varepsilon_{bR}}}R_b \tag{1}$$

where

$$\nu_{bR}=\frac{R_b}{E_b\varepsilon_{bR}} \tag{2}$$

is the limit coefficient of elasto-plasticity; ε_b is current concrete strain; ε_{bR} is peak concrete strain corresponding to the stress $\sigma_b(\varepsilon_{bR})=R_b$; R_b is compressive strength of concrete; E_b is the modulus of elasticity of concrete.

- Hognestad's [17] stress-strain curve

$$\sigma_b(\varepsilon_b)=\left(2\frac{\varepsilon_b}{\varepsilon_{bR}}-\left(\frac{\varepsilon_b}{\varepsilon_{bR}}\right)^2\right)R_b \tag{3}$$

- Bilinear stress-strain relationship

$$\sigma_b(\varepsilon_b)=\begin{cases}\varepsilon_b E_b^{sec1}\ ,\ \varepsilon_b E_b^{sec1}\le\eta R_b\\ \eta R_b+\left(\varepsilon_b-\dfrac{\eta R_b}{E_b^{sec1}}\right)E_b^{sec2}\ ,\ \text{otherwise,}\end{cases} \tag{4}$$

where

$$E_b^{sec1}=\nu E_b \tag{5}$$

$$E_b^{sec2}=\frac{E_b^{sec1}R_b(1-\eta)}{\varepsilon_{bR}E_b^{sec1}-\eta R_b} \tag{6}$$

ν is the coefficient of elasto-plasticity; η is the limit ratio of concrete stress and strength specifying almost elastic behaviour of cross section.

- The stress-strain relationship including the elasto-plastic effect

$$\sigma_b(\varepsilon_b)=\nu\varepsilon_b E_b \tag{7}$$

Actually, putting $\varepsilon_{bR}=2R_b/E_b$ into relation (1) we get Hognestad's formula (3). Such simplification can be treated as not sufficiently accurate because induces the same description of the character of plastic strain for various strength classes of concrete.

It is well known that deformational behavior of reinforced tensile concrete is different from the behavior of plain concrete. This distinction usually called tension stiffening can be explained, in the fact, that the stiffness of the cracked reinforced concrete between the consecutive cracks is higher than the stiffness of alone reinforcing steel.

Let us model tension stiffening by using the elementary smeared crack approach simulating the uncracked section by using ascending branch while descending branch of stress strain relation integrally reflects the tension stiffening effect

$$\sigma_{bt}(\varepsilon_{bt})=\begin{cases}\varepsilon_{bt}E_b\ ,\ \varepsilon_b E_b\le R_{bt}\\ \alpha R_{bt}-(\varepsilon_{bt}-\varepsilon_{btR})E_{bt}^{sec}\ ,\ \varepsilon_{btR}<\varepsilon_{bt}<\beta\varepsilon_{btR}\\ 0\ ,\ \varepsilon_{bt}\ge\beta\varepsilon_{btR}\end{cases} \tag{8}$$

where

$$E_{bt}^{sec}=\frac{\alpha R_{bt}}{\varepsilon_{btR}(\beta-1)} \tag{9}$$

$$\varepsilon_{btR}=\frac{R_{bt}}{E_b} \tag{10}$$

in which, ε_{bt} is average strain of tensile concrete; R_{bt} and ε_{btR} are tensile strength and cracking strain of concrete; α and β are the parameters integrally controlling the tension stiffening.

A linear stress strain behaviour of tensile steel mainly prevails at service load performance and stops approximately at 0.8-0.9M_u (where M_u is ultimate bending moment of the member) while compressive steel bars behave elastically even up to the element failure. Generally, plastic behaviour of reinforcement occurs near to the collapse of element when tensile concrete completely do not work. Consequently, for the reinforcing bars, a linear stress strain relationship in both tension and compression may be adopted

$$\sigma_s(\varepsilon_s)=\varepsilon_s E_s \tag{11}$$

where ε_s is average reinforcing bar strain; E_s is Young's modulus of reinforcement steel.

In addition, for approximate evaluation of plastic strain in tensile reinforcement the elasto-plastic diagram, similar to formula (7), can be also used.

2.3. Equilibrium

Consider a statically determined, doubly reinforced member in flexure (Fig. 1). Let us assume that shear forces and torsion do not significantly affect stiffness of the element cross-sections and can be omitted in non-linear formulation.

Relying on the above assumptions and requirements of the strain compatibility, the equilibrium equations can be expressed as

$$\begin{cases}\int\limits_{A_b}y\sigma_b(\varepsilon_b)dA+\int\limits_{A_{bt}}y\sigma_{bt}(\varepsilon_{bt})dA+\\ +\sigma_{s1}(\varepsilon_{s1})(h-a_1)A_{s1}+\sigma_s(\varepsilon_s)(h_0-a)A_s=M\\ \int\limits_{A_b}\sigma_b(\varepsilon_b)dA-\int\limits_{A_{bt}}\sigma_{bt}(\varepsilon_{bt})dA+\\ +\sigma_{s1}(\varepsilon_{s1})A_{s1}-\sigma_s(\varepsilon_s)A_s=0\end{cases} \tag{12}$$

where M is the external moment; A_b, A_{bt} and A_s, A_{s1} are the areas for compressive/tensile concrete and for the reinforcements, respectively; y is the distance to the neutral axis; $h_0 = h - a$ is an effective, while h is the overall depth of the cross-section; a_1 and a are distances between the centre of gravity of compressive and tensile reinforcements to the nearest edges of the cross-section (Fig. 1).

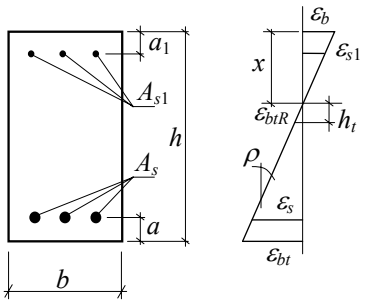

Fig. 1 RC beam cross-section and the average strain compatibility

2.4. Non-linear equations

In order to solve the system of equilibrium equation (12) relying on the above material models and assumtions, the following stages of deformational behavior of tension zone of RC member are initialized:

- the *uncracking* stage (i.e., $\varepsilon_{bt} \le \varepsilon_{btR}$);
- the *pure-tension stiffening* stage (i.e., $\varepsilon_{btR} < |\rho(h-x)| \le \beta\varepsilon_{btR}$);
- the *partially-tension stiffening* stage (i.e., $\varepsilon_{btR} < |\rho y| < \beta\varepsilon_{btR} \wedge |\rho(h-x)| > \beta\varepsilon_{btR}$);
- the *fully cracked* stage, when tensile concrete is neglected.

At the beginning of the uncracking stage the moment M and curvature ρ segment is a straight line defining elastic behaviour of RC cross-section. This stage is complete at the initiation of the first flexural crack when concrete deformation in extreme tensile fibre reaches its ultimate tensile deformation ε_{btR}. At pure and partially tension-stiffening stages the behavior of the block of tensile concrete between consecutive cracks significantly affect the moment-curvature relation while the fully cracked stage occurs when RC cross section works near to the failure moment.

Omitting the behaviour of the uncracked cross-section consider more important stage of pure tension stiffening. Substituting relationship (8) for tensile concrete and relation (11) for both tensile and compressive reinforcements into the system of equations (12) we obtain the following system of nonlinear equations

$$\begin{cases} \dfrac{bE_{bt}^{sec}}{\rho^2}\left(\dfrac{\varepsilon_{btR}\beta}{2}\left((h-x)^2\rho^2-\varepsilon_{btR}^2\right)-\dfrac{1}{3}\left((h-x)^3\rho^3-\varepsilon_{btR}^3\right)\right)+ \\ +\dfrac{bE_b\varepsilon_{btR}^3}{3\rho^2}+\rho E_s\left((h_0-x)^2A_s+(x-a_1)^2A_{s1}\right)+M_b=M \\ \dfrac{bE_{bt}^{sec}}{\rho}\left(\dfrac{1}{2}\left((h-x)^2\rho^2-\varepsilon_{btR}^2\right)-\varepsilon_{btR}\beta\left((h-x)\rho-\varepsilon_{btR}\right)\right)- \\ -\dfrac{bE_b\varepsilon_{btR}^2}{2\rho}-\rho E_s\left((h_0-x)A_s+(x-a_1)A_{s1}\right)+F_b=0 \end{cases} \tag{13}$$

where ρ is load induced curvature while F_b and M_b are internal force and internal moment of concrete compressive zone about the neutral axis.

Similarly, the system of nonlinear equations for the partially tension-stiffening stage is expressed as

$$\begin{cases} \dfrac{bE_{bt}^{sec}\varepsilon_{btR}^3}{\rho^2}\left(\dfrac{1}{2}\beta\left(\beta^2-1\right)-\dfrac{1}{3}\left(\beta^3-1\right)\right)+\dfrac{bE_b\varepsilon_{btR}^3}{3\rho^2}+ \\ +\rho E_s\left((h_0-x)^2A_s+(x-a_1)^2A_{s1}\right)+M_b=M \\ \dfrac{bE_{bt}^{sec}\varepsilon_{btR}^2}{\rho}\left(\dfrac{1}{2}\left(\beta^2-1\right)-\beta\left(\beta-1\right)\right)-\dfrac{bE_b\varepsilon_{btR}^2}{2\rho}- \\ -\rho E_s\left((h_0-x)A_s+(x-a_1)A_{s1}\right)+F_b=0 \end{cases} \tag{14}$$

The fully cracked stage of RC member can be modeled by the following equations:

$$\begin{cases} M_b+\rho E_s\left(A_s(h_0-x)^2+A_{s1}(x-a_1)^2\right)=M \\ F_b-\rho E_s\left(A_s(h_0-x)+A_{s1}(x-a_1)\right)=0 \end{cases} \tag{15}$$

The internal force F_b and moment M_b reflecting the behavior of concrete compressive zone are derived in explicit form. For prEN 1992–1's [1] stress strain diagram (1) are obtained the following formulae

$$M_b=\frac{1}{2}\frac{bR_bz_c^2x^2}{z_b^2}-\frac{1}{3}\frac{bR_b^2x^3\rho}{z_b\varepsilon_{bR}}-\frac{bR_b^2\varepsilon_{bR}z_c^2x}{z_b^3\rho}+ \\ +\frac{bR_b^3\varepsilon_{bR}^2\left(-z_c\right)^2\left(ln\left(z_a\right)-ln\left(R_b\varepsilon_{bR}\right)\right)}{z_b^4\rho^2} \tag{16}$$

$$F_b=\frac{bR_bz_c^2x}{z_b^2}-\frac{1}{2}\frac{bR_b^2x^2\rho}{z_b\varepsilon_{bR}}+ \\ +\frac{bR_b^2\varepsilon_{bR}z_c^2\left(ln\left(R_b\varepsilon_{bR}\right)-ln\left(z_a\right)\right)}{z_b^3\rho} \tag{17}$$

where

$$z_a=R_b\varepsilon_{bR}+x\rho z_c \tag{18}$$

$$z_b=-2R_b+E_b\varepsilon_{bR} \tag{19}$$

$$z_c=-R_b+E_b\varepsilon_{bR} \tag{20}$$

When stress strain diagram is defined by Hognestad's [17] diagram (3) the explicit form of F_b and M_b is the following

$$M_b=\frac{1}{12}\frac{bR_bx^3\rho\left(8\varepsilon_{bR}-3x\rho\right)}{\varepsilon_{bR}^2} \tag{21}$$

$$F_b=\frac{1}{3}\frac{bR_bx^2\rho\left(3\varepsilon_{bR}-x\rho\right)}{\varepsilon_{bR}^2} \tag{22}$$

The internal moment and force of concrete compressive zone for bilinear stress strain diagram (4) is derived in the form

$$M_b=\begin{cases}\dfrac{1}{3}bx^3\rho E_b^{sec1},\ \sigma_b\le\eta R_b\\ \dfrac{b\left(\eta R_b\right)^3}{3\rho^2\left(E_b^{sec1}\right)^2}+\dfrac{b}{\rho^2}\left[\dfrac{1}{3}E_b^{sec2}\left(x^3\rho^3-\left(\dfrac{\eta R_b}{E_b^{sec1}}\right)^3\right)+\right.\\ \left.+\dfrac{1}{2}\left(\eta R_b-\dfrac{\eta R_b E_b^{sec2}}{E_b^{sec1}}\right)\left(x^2\rho^2-\left(\dfrac{\eta R_b}{E_b^{sec1}}\right)^2\right)\right]\end{cases} \quad (23)$$

$$F_b=\begin{cases}\dfrac{1}{2}bx^2\rho E_b^{sec1},\ \sigma_b\le\eta R_b\\ \dfrac{1}{2\rho}b\dfrac{\left(\eta R_b\right)^2}{E_b^{sec1}}+\dfrac{b}{\rho}\left[\dfrac{1}{2}E_b^{sec2}\left(x^2\rho^2-\left(\dfrac{\eta R_b}{E_b^{sec1}}\right)^2\right)+\right.\\ \left.+\left(\eta R_b-\dfrac{\eta R_b E_b^{sec2}}{E_b^{sec1}}\right)\left(x\rho-\dfrac{\eta R_b}{E_b^{sec1}}\right)\right]\end{cases} \quad (24)$$

Considering the stress strain diagram (7), F_b and M_b may be evaluated in the following way. The coefficient ν completely characterizes the elasto-plastic properties of concrete under axial compression and can be obtained directly from the prism tests. When an element is subjected to bending the character of stress strain diagram is unknown because the stress distribution within the element depth cannot be measured directly from experiments. Therefore, following [18], the coefficient of the diagram shape for compressive concrete ω is adopted in the current analysis. In particular, if the loading begins the compressive zone of RC member behaves similarly to elastic material, and $\omega\approx 0.5$, $\nu\approx 1$ can be assumed. With increasing the intensity of loading, plastic deformation occurs and the stress strain diagram becomes similar to a rectangle, then the coefficient ω is tending to 1, while $\nu\to\nu_{bR}$. According to [18], these coefficients become $\omega\approx 1$ and $\nu\approx 0.45$ in the service-load performance. It should be noted that in both mentioned cases the product of these coefficients remains approximately constant.

Consequently, the internal moment of compressive zone and its internal force may be calculated by the formulae

$$M_b=\nu\omega\rho bx^3E_b\omega^* \quad (25)$$

$$F_b=\nu\omega\rho bx^2E_b \quad (26)$$

where $\omega^*=2/3$ for triangular diagram while $\omega^*=1/2$ for rectangular diagram.

According to the regulations [3] about the linear-instantaneous creep deformation, the coefficient may be evaluated by using $\nu\approx 0.85$. In particular, for the triangle diagram the product of coefficients $\nu\omega\omega^*$ is equal to 0.28 while for the rectangular diagram $\nu\omega\omega^*=0.23$. Thus, this difference is relatively small. In addition, according to [18], the diagram of compressive stress of concrete in experimental RC beam tests up to the level $\sigma_b/R_b\le 0.6$ is similar to the triangle.

2.5. Investigations of the solvability

The equilibrium relations (13)-(15) may be considered as two-variable function $M(x,\rho)$ subjected to the plane of cracking moment M_c and the failure moment M_u. As an example, the graphs of these functions (Fig. 2) are computed for slightly reinforced (reinforcement ratio) ($\mu=0.47\%$) and for normally reinforced ($\mu=1.5\%$) members with the cross-section of 150x400 mm (Fig. 2). Compressive strength of concrete prism R_b=35 MPa, tensile strength R_{bt}=2.9 MPa, coefficient of elasto-plasticity $\nu=0.8$, the values of parameters α and β are given in Section 3.

Not considering the equations of force balance the surfaces $M(x, \rho)$, depicted in (Fig. 2), may be primarily treated as the possible root functions. As can be seen in Fig. 2, b, plastic strains of compressive concrete, modeled by putting relations (16) and (21) into systems (13)-(14), induce the possible solutions on both the ascending and descending surfaces if the bending moment tends to M_u. These graphs also show that the degree of nonlinear equations (13)-(14), taking into account relationships (21) and (16), is higher than the degree of these equations relying on expression (25). Moreover, the descending surfaces are not occurring even up to the failure for slightly reinforced member.

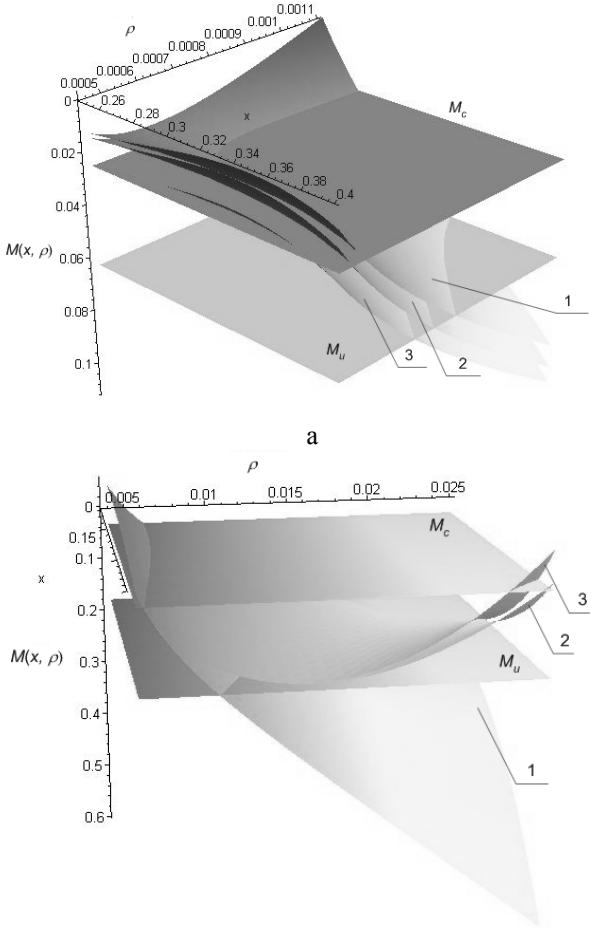

Fig. 2 Moment-curvature-neutral axis surfaces for slightly (a) and for normally (b) reinforced members. M_b calculated by: *1*- eq. (25); *2* - eq. (21); *3* - eq. (16)

The substitution of force equilibrium relation into

the equation for moment balance gives a polynomial of the degree n in x. In particular, Table 1 shows that the degree of the equations (13)-(14) varies over the range of 6-9 and, according to Abel's theorem [10], the explicit solutions in terms of radicals for these equations do not exist. Therefore, the problem of modeling of RC cracked members concentrates on the application of implicit approaches.

Table 1

Degree of a polynomial in the location of neutral axis

Diagram	Degree n for the stages		
	Tension stiffening		Fully cracking
	Pure	Partial	
prEN 1992–1's (1)	9	9	5
Hognestad's (3)	9	9	5
Bilinear (4)	8	6	6
Elasto-plastic (7)	6	6	2

In addition, it has been established that all solutions of the problems (13)-(14) taking into account relations (16)-(17) and (21)-(22) cannot be obtained by using elementary Newton's step-by-step procedure. Local convergence mainly occurs for the elements with normal and high reinforcement ratios working near to the failure loads. In particular, this aspect is proved also in [7] where it has been established that in non linear analysis of RC members exist non smooth and non-convex regions, which result in the multiplied solutions, ie several stress and strain states may correspond to the same load condition depending on the loading history. This can be even if the stress strain relationships used for concrete and reinforcement has no descending branches [7].

In order to reduce the degree of the problem (13) enabling us to find the explicit solution, the depth of uncracked tensile cross-section zone, h_t (Fig. 1) depending on acting moment is adopted

$$h_t = \frac{\varepsilon_{btR}}{\rho_{cr}} - \left(\frac{M - M_c}{M_{pr,stf} - M_c}\right)^k \frac{\varepsilon_{btR}\beta - \rho_{cr}\left(h - x_{pr,stf}\right)}{\rho_{cr}\beta} \quad (27)$$

where ρ_{cr} is the curvature induced by cracking moment M_c; $M_{pr,stf}$ and $x_{pr,stf}$ are the moment and location of the neutral axis specifying the end of pure tension stiffening stage when deformation in extreme tensile fibre reaches its ultimate value $\varepsilon_{btR}\beta$; k is the index, if k=1, then h_t is defined by linear interpolation.

Now, the system of equations (13) in terms of h_t may be rewritten as follows:

$$\begin{cases} bE_{bt}^{sec}\left(\frac{1}{2}\varepsilon_{btR}\beta\left((h-x)^2 - h_t^2\right) - \frac{1}{3}\left((h-x)^3\rho - h_t^3\rho\right)\right) + \\ + \frac{bE_b\rho h_t^3}{3} + \rho E_s\left((h_0 - x)^2 A_s + (x - a_1)^2 A_{s1}\right) + M_b = M \\ bE_{bt}^{sec}\left(\frac{1}{2}\left((h-x)^2\rho - h_t^2\rho\right) - \varepsilon_{btR}\beta\left((h-x) - h_t\right)\right) - \\ - \frac{bE_b\rho h_t^2}{2} - \rho E_s\left((h_0 - x)A_s + (x - a_1)A_{s1}\right) + F_b = 0 \end{cases} \quad (28)$$

Putting into the system (28) expressions (25) and (26) we obtain the polynomial of the forth degree in the location of neutral axis x and we can derive the solution of this system in explicit form.

The influence of the adopted formula (27) on the moment-curvature diagram for different strength grades C of concrete and reinforcement ratios μ is investigated by comparing results obtained by solving the system (28) with those derived from the system (13). The comparative surfaces depicted in Fig. 3 show that the numerical solution of (13), denoted by ρ_{num}, differs from solution of (28) (denoted by ρ_{approx}) taking into account the approximation (27) over the range of 0.94-1.05. As can be seen in Fig. 3 these upper and lower errors are sufficiently small and occur if the member is slightly reinforced and acting moment M tends to the moment of cracking M_c while $M \to M_u$ these differences remain about 1. Finally, the numerical solution has been obtained by using a genetic algorithm technique [5]. Cross-section of the member is assumed to be 150x400 mm. Index k in expression (27) assumed to be 0.5 on the basis of tests data analysis presented in Section 3. The values of the parameters α and β are also given in Section 3.

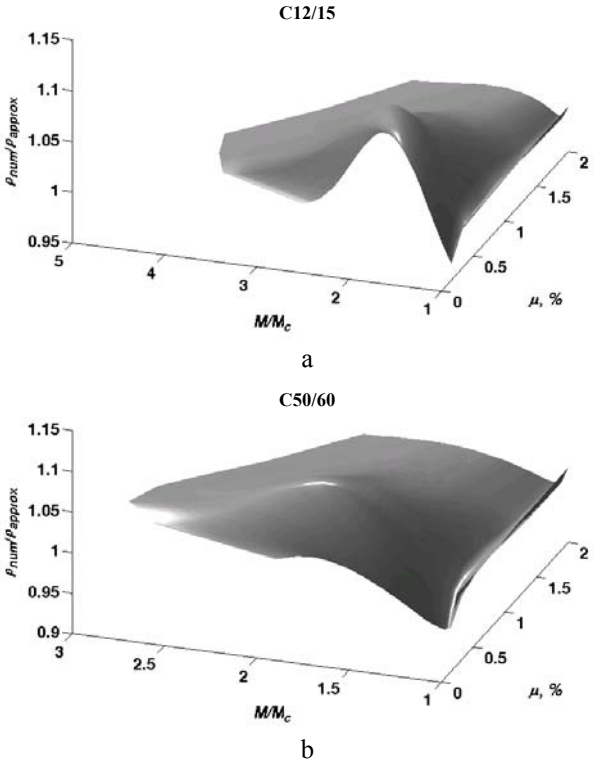

Fig. 3 Comparative surfaces of dimensionless approximated (28) and numerically computed curvatures (13) vs reinforcement and moment ratios

As stated in Table 1, the location of neutral axis for the fully cracked cross-section can be simply derived from quadratic equation inserting (25) and (26) into (15). This derivation is generalized in terms of an effective moment of inertia I_{cr}^{eff} about the neutral axis and is expressed as

$$\rho = \frac{M}{E_b I_{cr}^{eff}}, \quad I_{cr}^{eff} > 0, \quad I_{cr}^{eff} \in \boldsymbol{R} \quad (32)$$

where

$$I_{cr}^{eff} = \nu\omega b x^3 \omega^* + n_c\left((x-a_1)^2 A_{s1} + (h_0 - x)^2 A_s\right) \quad (33)$$

$$x = x_{1,2} = \frac{-A_{s,red} \pm \sqrt{A_{s,red}{}^2 + 4b\omega\nu S_{s,red}}}{2b\omega\nu} \quad (34)$$

$$A_{s,red} = n_c\left(A_s + A_{s1}\right) \quad (35)$$

$$S_{s,red} = n_c\left(A_s h_0 + A_{s1} a_1\right) \quad (36)$$

in which $A_{s,red}$ and $S_{s,red}$ are the reinforcement area and the first moment of this area about top surface of the cross-section transformed to the concrete by using the ratio $n_c = E_s / E_b$.

The fully cracked section stage is complete when bending moment M reaches its ultimate value $M_u = \rho_u E_c I_{cr}^{eff}$. The latter is determined by ultimate curvature ρ_u that specifies the failure mode because of concrete crushing or the collapse because of steel bars breaking.

In order to compare (33) with code's [3] curvature relation we rearrange the latter into the following expression of an effective moment of inertia:

$$I_{cr}^{eff} = \frac{h_0 z}{\left(\frac{\psi_s}{\alpha A_s} + \frac{\psi_b}{bx\nu}\right)} \quad (37)$$

where z is empirical-based distance from the center of tensile reinforcement A_s to the resultant of compressive zone diagram; ψ_s is the coefficient averaging tensile deformations evaluating the tension stiffening effect; ψ_b is the averaging coefficient of compressive concrete deformations over the cracked span of the beam.

Thus, the graphs of effective moments of inertia (33) and (37) with respect to triangular and rectangular stress strain diagrams of compressive concrete and the reinforcement ratio are shown in Fig. 4. For the triangular diagram the coefficient ν is assumed to be 0.8 while for the rectangular diagram this coefficient accepted to be 0.4.

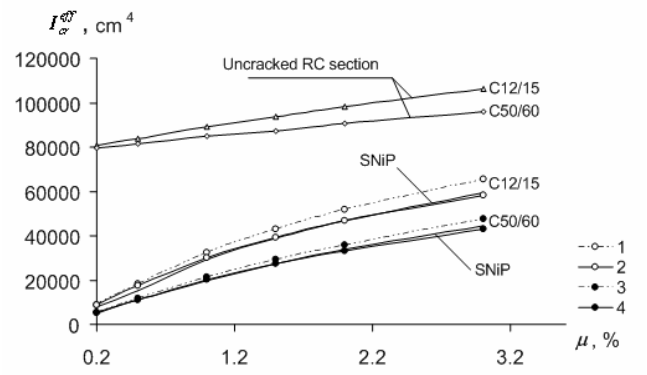

Fig. 4 Effective moment of inertia of fully cracked and uncracked cross sections: *1*, *3* - for triangular stress strain diagram of compressive concrete; *2*, *4* - the same for rectangular diagram

The graphs of Fig. 4 quantitatively show the degradation of the inertia moment from uncracked up to fully cracked cross-section. As can be seen, the values obtained by (33) relation are very close to those calculated by SNiP formula (37) if the rectangular diagram of compressive concrete is applied. In computations, the fully cracked stage is assumed to be at the loading level $M = 0.8 M_u$, accordingly, $\psi_s = 1$.

3. Experimental verification

The further experimental verification of the method proposed is focused on the explicit solution of the system (28) taking into account proposed formula (27), for the pure tension-stiffening stage, and the numerical solution of the system (14), for the partially tension stiffening stage, by applying formulae (25) and (26) for these purpose. The obtained formula (33) is also employed in the analysis.

The experimental verification have been performed by comparing analytical and test values of the moment-curvature as well as the moment-depth of uncracked tensile cross-section zone functions in pure bending of RC members. In such a way, the proposed approach is approved for the extensive range of loading levels and different reinforcement ratios of the beams. The empirical-based method [3] was also employed in comparative analysis.

Let us briefly describe physical properties of concrete which were implemented in the analysis. The governing parameter β controlling the effects of tension stiffening has been investigated by various investigators particularly in shear or tension tests using its range within 5 and 20. Despite of the fact that various parameters affect the character of tensile stress strain relation, a quantitative dependence between the length of the unloading branch and the reinforcement ratio, recently, has been derived from experimental RC beam in bending [19]

$$\beta = \begin{cases} 7.12\mu^2 - 27.6\mu + 32.8, & \text{if } \mu < 2 \\ 6\,, & \text{otherwise} \end{cases} \quad (38)$$

where

$$\mu = \frac{A_s + A_{s1}}{bh_0} 100\% \quad (39)$$

The switching between triangular ($\nu = 0.8$) and rectangular ($\nu = 0.4$) diagram of concrete in compression is performed when the stress intensity factor σ_b / R_b reaches its value equal to 0.6.

Thus, the method proposed is applied to the extensive experimental data reported by Nemirovskyi and Kochetkov in [20]. They have tested RC beams with 0.2, 0.4, 0.9 and 1.5% reinforcement ratios under short- and long-term loading. The compressive strength tested on 100 mm edges length cubes was in the range 55-61.4 MPa. All 150x400 mm cross-section and 400 cm of the span length beams were tested under a four-point loading system that gave a constant moment zone of 1/3 span. Concrete strains have been measured accurately throughout all the length of the pure bending zone by using 12 tensometric gauges lines located at the different depths of the beam. The average strains of the reinforcement and concrete were additionally controlled by the clock-type indicators with the basis length of 250, 500, 800 mm. The reinforcement

strain was also controlled using the uninterrupted tensometric gauge line embedded within the reinforcement bars. The moment of cracking has indicated not only in the visual way, but also by the indications of the mentioned gauge line. The rest data used in present analysis was taken from research [20].

The adequacy of the experimental (Series BII-1, BII-2, BIII-3) values of h_t and their theoretical equivalent calculated by the proposed formula (27) is depicted in Fig. 5. As it can be seen, the character of depth h_t distribution is nonlinearly dependent on the reinforcement ratio and bending moment M, i.e. increasing the bending moment the depth of uncracked tensile cross-section suddenly decreases and.this diminution is more intensive for slightly reinforced beams. The graphs depicted in Fig. 5 show that the proposed relation sufficiently accurately reflects the results of experimental test data. These results were obtained using the index k to be 0.5.

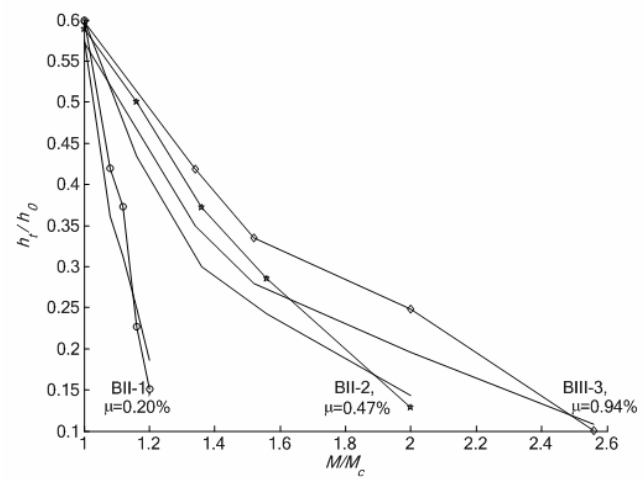

Fig. 5 Relative depth of uncracked tensile concrete zone of RC beams reinforced by the ratio μ vs the relative bending moment

Fig. 6 - Fig. 9 show comparative graphs of the calculated and measured [20] values of curvature ρ versus bending moment M for the cracked RC beams with various longitudinal reinforcement ratios μ . These results can be treated as sufficiently accurate for the beams with reinforcement ratio over the range of 0.2-1.5%.

Finally, it should be stated that code SNiP [3] gives rather conservative predictions of the curvature. Due to the bond with reinforcement, the concrete between cracks caries a certain amount of tensile force normal to the cracked plane and contributes to overall stiffness of the member. This fact is very important for the slightly reinforced beams and we can see (Fig. 6 -Fig. 7) that the curvature predictions made by SNiP method for such beams may be treated as insufficient. In this case, the method proposed enables us to perform more accurate deformational analysis of RC flexural members.

In summary, the obtained results show that pure tension stiffening stage occurring in slightly reinforced members can spread throughout cracking even up to failure resulting in nonlinear moment-curvature diagram. Normally reinforced concrete elements mainly work in the stages of partial tension stiffening and full cracking, while the pure tension stiffening stage occurs if acting moment is slightly higher than the moment of cracking M_{cr}. In general, RC beams working on partially tension-stiffening or fully cracked stages have almost linear M-ρ relation and, therefore, all of the compared methods reflect quite adequate conformity of the calculated and the tests results. Accordingly, the simple linear interpolation between the curvature specifying the end of pure tension stiffening stage and the curvature of fully cracked cross-section may be also used in the analysis RC flexural members. Furthermore, the obtained results have also proved that for beams with the reinforcement ratio higher than 1.5% the tension stiffening effect can be completely ignored performing the calculations for fully cracked cross-section using equation (32) throughout the cracking up to the almost failure.

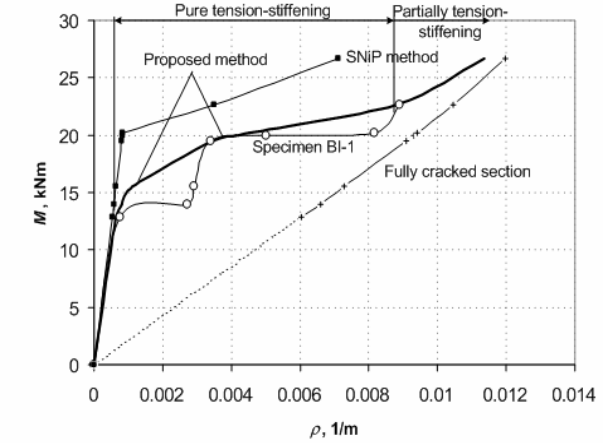

Fig. 6 Calculated and measured curvatures of cracked RC beam (Series BI-1, μ=0.2%)

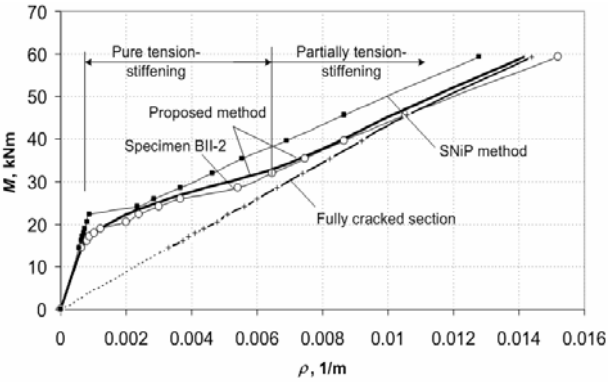

Fig. 7 Calculated and measured curvatures of cracked RC beam (Series BII-2, μ=0.5%)

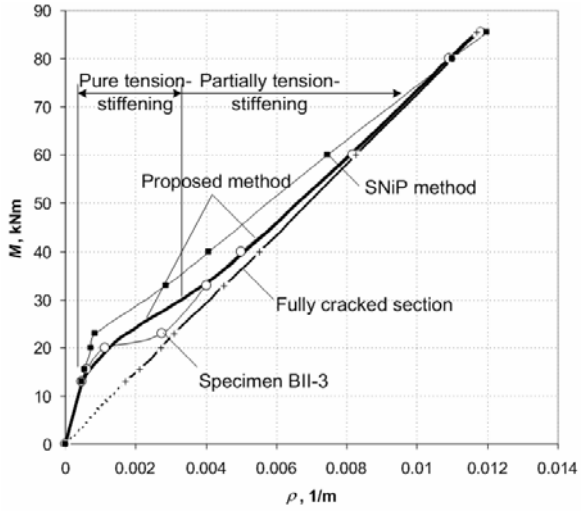

Fig. 8 Calculated and measured curvatures of cracked RC beam (Series BII-3, μ=0.9%)

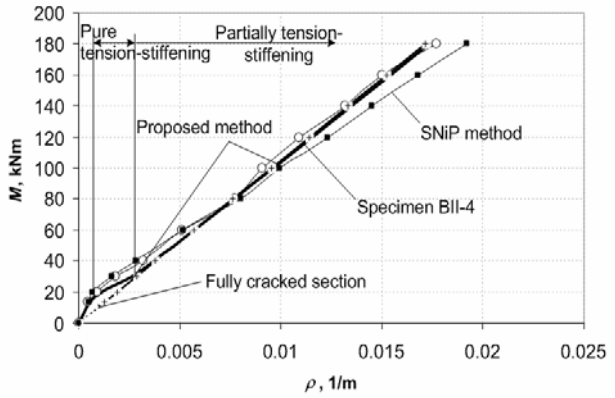

Fig. 9 Calculated and measured curvatures of cracked RC beam (Series BII-4, μ=1.5%)

4. Concluding remarks

Instead of using the layer approach, relevant to the difficulties of inaccurate dividing of concrete and reinforcement cross-sections into horizontal stripes, inconvenient processes of iteration convergence checking for each and all the layers changing their elastic stiffness, as well as the approximate searching of the location of neutral axis by the layer strains; the semi analytical modeling of RC members in bending has been proposed. The method uses the explicit (without the need of numerical integration) derivation of internal forces and moments, for compressive concrete, applying the second-degree Hognestad's, prEN 1992-1's parabolas as well as the bilinear, and linear elasto-plastic stress strain diagrams while, for concrete in tension, employing the smeared cracks approach. In order to find the explicit solution of the system of nonlinear equations in terms of curvature and the neutral axis there can be used the proposed relation between acting moment and the depth of the zone of uncracked tensile cross-section in combination with elasto-plastic stress strain diagram for concrete in compression. The proposed relationships are found to be of an adequate accuracy through the analysis of numerical examples and experimental verification of curvatures of cracked RC concrete members with reinforcement ratio varying in the range from 0.2 to 1.5%.

References

1. prEN 1992–1 (Final draft). EuroCode 2: Design of Concrete Structures. -European Committee for Standardization, October, 2001.-230p.
2. ACI Committee 318: Building Code Requirements for Reinforced concrete (ACI 318-99/ACI 318R-95).-Michigan: American Concrete Institute (ACI), 1996. -300p.
3. СНиП 2.03.01-84*. Бетонные и железобетонные конструкции. -Москва: Госстрой СССР, 1989.-80с.
4. **Sato, R., Xu, M., Ujike, I.** Effect of tension softening on time–dependent deformation and crack width of reinforced concrete flexural members. -Proc. FRAMCOS–3. -Freigurg: AEDIFICATIO Publishers D–79104, 1998, p.1341-1352.
5. **Balevičius, R., Simbirkin, V.** Modeling of physical nonlinearity of reinforced concrete elements under long-term loading. -Mechanika. -Kaunas: Technologija, 2003, Nr.4(42), p.19-26.
6. **Wu, Y., Luna, R.** Numerical implementation of temperature and creep in mass concrete. -Finite Elements in Analysis and Design, 2001, No37, p.97-106.
7. **Алявдин П. В.**, **Симбиркин В. Н.** Решение негладких задач расчета элементов железобетонных конструкций. -Будаўніцтва. -Строительство. -Construction, 2001, No1, с.11-21.
8. **Romero, M.L., Miguel, P.F., Cano, J.J.** A parallel procedure for nonlinear analysis of reinforced concrete three-dimensional frames. -Computers and Structures, 2002, 80, p.1337-1350.
9. **Crisfield, M.A.** Local instabilities in the non-linear analysis of reinforced concrete beams and slabs. -Proc. Instn. Civ. Engrs. Part 2, 2002, v. 73, p.135-145.
10. **Алексеев В. Б.** Теорема Абеля в задачах и решениях. -Москва: МЦНМО, 2001.-192с.
11. **Розенблюмас А.** Расчет армированных бетонных конструкций с учетом растягивающих напряжений в бетоне. -Исследования по железобетонным конструкциям I.-Вильнюс: Минтис, 1966, с.3-32.
12. **Mendis, P.A., Darval, P.I.** Stability analysis of softening frames.-J. of Structural Engineering, 1988, v.114, No5, p.1057-1072.
13. **Sheikh, S.A., Yeh, C.C.** Analytical moment curvature relations for tied concrete columns. -J. of Structural Engineering, 1992, v.118, No2, p.529-544.
14. **Rodriguez-Gutierrez, J.A., Aristizabal-Ochoa, J.D.** *M–P–Φ* diagrams for reinforced, partially and fully prestressed concrete sections under biaxial bending and axial load. -J. of Structural Engineering, 2001, v.127, No7, p.763-773.
15. **Hsu, T.T.C.** Towards a unified nomenclature for reinforced concrete theory. -J. of Structural Engineering, 1996, v.122, No3, p.275-283.
16. **Rashid, Y.R.** Analysis of prestressed concrete pressure vessels. -Nuclear Engineering Design, 1968, v.7, No4, p.334-344.
17. **Hognestad, E.A.** Study of combined bending and axial load in reinforced concrete members. -Bulletin 399. -University of Illinois Engineering Experiment Station, Urbana III, 1951.-128p.
18. **Залесов А.С., Кодыш Э.Н., Лемыш Л.Л., Никитин И.К.** Расчет железобетонных конструкций по прочности, трещиностойкости и деформациям. -Москва: Стройиздат, 1988.-320с.
19. **Kaklauskas, G., Ghaboussi, J.** Stress-strain relations for cracked tensile concrete from RC beam tests. -J. of Structural Engineering, 2001, v.127, No1, p.64-73.
20. **Немировский Я.М., Кочетков О.И.** Влияние работы растянутой и сжатой зон бетона на деформации обычных изгибаемых железобетонных элементов после возникновения в них трещин.-Особенности деформаций бетона и железобетона и использование ЭВМ для оценки их влияния на поведение конструкций. -Москва: НИИЖБ, 1969, с.106-156.

R. Balevičius

PUSIAU ANALITINIS LENKIAMŲ GELŽBETONIO ELEMENTŲ MODELIAVIMAS

R e z i u m ė

Straipsnyje lenkiamų gelžbetonio strypinių ele-

mentų modeliavimui taikomos tikslios skerspjūvio vidinių jėgų ir momentų lygtys, atsisakant skaitinio integravimo metodų. Naudojant vidutinių plyšių modelį tempiamam betonui bei įvairias gniuždomo betono įtempių ir deformacijų diagramas, ištirtos netiesinių lygčių analitinio sprendžiamumo galimybės. Rezultatai, gauti taikant pasiūlytos priklausomybes, palyginti su rezultatais, gautais taikant empirinę SNiP normų metodiką. Atlikti skaitiniai eksperimentai, parodytas teorinių ir eksperimentinių dydžių adekvatumas.

R. Balevičius

SEMI ANALYTICAL MODELLING OF REINFORCED CONCRETE MEMBERS IN BENDING

S u m m a r y

In present research, the proposed technique has been focused on explicit derivation of internal forces and moments for reinforced concrete in tension and compression without the need of numerical integration. The application of different stress strain relations for compressive concrete and the smeared crack approach for tensile concrete is investigated on the basis of an opportunity to find the explicit solution of nonlinear equations. The approach proposed is found to be effective by numerical examples, and an adequate accuracy of the analysis results in comparison with the experimental data.

Р. Балявичюс

ПОЛУАНАЛИТИЧЕСКОЕ МОДЕЛИРОВАНИЕ ЖЕЛЕЗОБЕТОННЫХ ИЗГИБАЕМЫХ ЭЛЕМЕНТОВ

Р е з ю м е

В статье представлен анализ моделирования железобетонных элементов при изгибе с учетом концепции усредненных трещин и диаграмм деформирования материалов. Зависимости между усилиями и напряжениями, деформациями и жесткостями строились на основе возможностей их аналитического решения. Предложенная расчетная методика апробирована в результате численных исследований и путем сопоставления результатов расчета с экспериментальными данными, а также с методом СНиПа.

Received February 23, 2005

DOI: 10.5755/j02.mech.14504